Geomechanics and Engineering, *Vol. 22, No. 6 (2020) 519-528*
DOI: https://doi.org/10.12989/gae.2020.22.6.519

Modeling the wetting deformation behavior of rockfill dams

Wanli Guo[1a], Ge Chen[*2], Yingli Wu[1b] and Junjie Wang[3c]

[1]*Geotechnical Engineering Department, Nanjing Hydraulic Research Institute, Nanjing 210024, China*
[2]*Key Laboratory of Ministry of Education for Geomechanics and Embankment Engineering, Hohai University, Nanjing, Jiangsu 210098, China*
[3]*Key Laboratory for Hydraulic and Waterway Engineering of Ministry of Education, Chongqing Jiaotong University, Chongqing 400074, China*

(Received October 25, 2019, Revised July 31, 2020, Accepted August 18, 2020)

Abstract. A mathematical wetting model is usually used to predict the deformation of core wall rockfill dams induced by the wetting effect. In this paper, a series of wetting triaxial tests on a rockfill was conducted using a large-sized triaxial apparatus, and the wetting deformation behavior of the rockfill was studied. The wetting strains were found to be related to the confining pressure and shear stress levels, and two empirical equations, which are regarded as the proposed mathematical wetting model, were proposed to express these properties. The stress and deformation of a core wall rockfill dam was studied by using finite element analysis and the proposed wetting model. On the one hand, the simulations of the wetting model can estimate well the observed wetting strains of the upstream rockfill of the dam, which demonstrated that the proposed wetting model is applicable to express the wetting deformation behavior of the rockfill specimen. On the other hand, the simulated additional deformation of the dam induced by the wetting effect is thought to be reasonable according to practical engineering experience, which indicates the potential of the model in dam engineering.

Keywords: dams; wetting deformation; finite-element modeling; rockfills

1. Introduction

Core wall rockfill dams, using compacted rockfill materials within the dam body and a vertical or inclined clay core wall as the impermeable system, are a widely used dam type around the world (Oldecop and Alonso 2007, Ameen *et al.* 2017, Pramthawee *et al.* 2017). In addition, rockfill materials, which are widely used in rockfill dams, usually undergo many complicated conditions (Tao *et al.* 2019, Sukkarak *et al.* 2018). Investigations involving the rockfill material have focused primarily on its mechanical and engineering behavior using a saturated triaxial test (Xiao *et al*. 2017, Raksiri *et al.* 2018, Memduh and Murat 2019, Javad *et al.* 2019). It is well recognized that the rockfill materials of the upstream dam shell will experience "dry" to "wet" conditions during and after water storage. Progressive weathering, breakage and rearrangement of the rockfill particles will occur during wetting, which may subsequently lead to additional deformation in the dam body even if the stress is kept constant (Fu *et al.* 2011). Significant deformation occurs due to the wetting effect of the rockfills, which is known as "wetting deformation" (Chen *et al.* 2011).

∗Corresponding author, Ph.D.
E-mail: gechenhhu@163.com
[a]Ph.D.
E-mail: guowljs@163.com
[b]Ph.D.
E-mail: wuyingli@nhri.cn
[c]Ph.D.
E-mail: wangjunjiehhu@163.com

New constitutive models have been proposed to model the wetting effect, such as modeling the wetting deformation of stressed and moisture-sensitive weathered rockfill materials in a simplified manner by degrading the solid hardness (Escuder *et al.* 2005, Bauer *et al.* 2010, Fu *et al.* 2011). These constitutive models, capable of predicting the stress and deformation behavior during loading and creeping in a unified manner, are more theoretical and undoubtedly reasonable. However, many researchers and engineers have been accustomed to using classical and well-known constitutive models in the numerical analysis of dams, such as the Cam-Clay and Duncan-Chang's *E-B* and *E-v* models, which cannot consider the wetting deformation of rockfills. Therefore, another widely used method is to establish mathematical wetting models through a wetting test. The stress and strain components can be estimated by, e.g., Duncan-Chang's *E-B* model, and translated into the initial stress condition, which are further applied to the finite elements to obtain the wetting deformation of the dam by adding the mathematical wetting model. Despite the ignorance of the physical background underlying wetting deformation in the mathematical wetting models, this method is still widely used in dam engineering in China due to its practicality. Some wetting models obtain stress relaxation in the wetting process, such as the study of Reza *et al* (2015) and Zhou *et al* (2019), and the relaxation stress is regarded as the initial stress to simulate the wetting deformation. Meanwhile, some other wetting models are strain-based, and the wetting strain is regarded as the initial strain to simulate the wetting deformation. For example, the typical and widely used wetting model in China is expressed as follows (Li *et al.* 2004):

ISSN: 2005-307X (Print), 2092-6219 (Online)

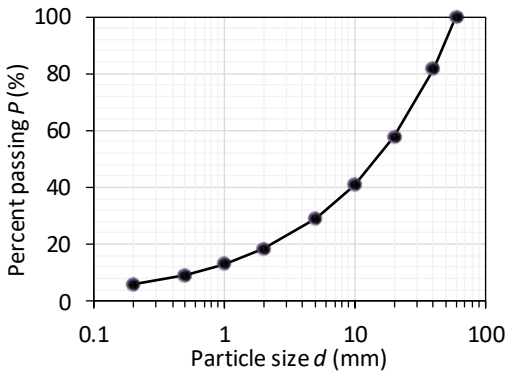

Fig. 1 Particle size distribution of the HPR

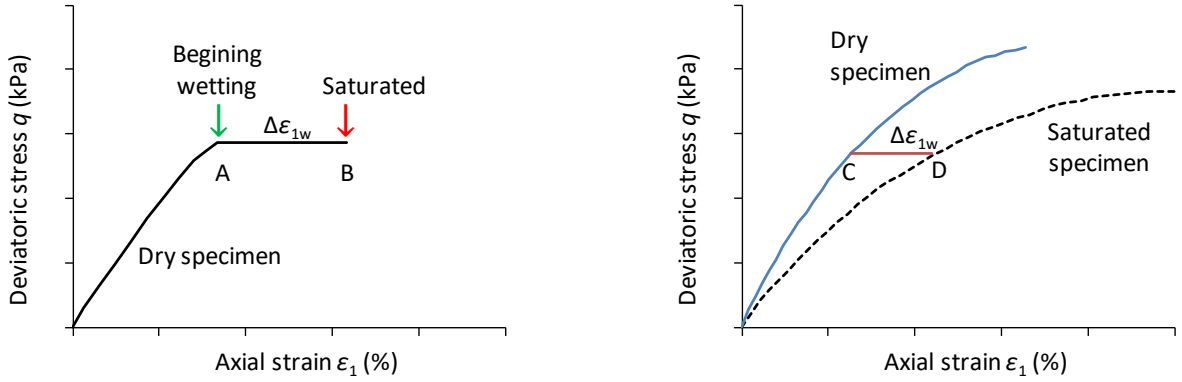

(a) Single-line method (b) Double-line method

Fig. 2 Commonly used wetting triaxial test methods

$$\begin{cases} \Delta\varepsilon_{vw} = c_w \left(\dfrac{\sigma_3}{p_a} \right)^{n_w} \\ \Delta\varepsilon_{sw} = b_w \dfrac{s}{1-s} \end{cases} \tag{1}$$

where c_w, n_w and b_w are the material constants, σ_3 is the confining pressure, p_a is the atmosphere pressure, and $\Delta\varepsilon_{vw}$ and $\Delta\varepsilon_{sw}$ are the wetting volumetric strain and wetting shear strain, respectively. The stress level s is known as the ratio of the current deviatoric stress q and the peak deviatoric stress q_f:

$$s = \frac{q}{q_f} \tag{2}$$

where $0 \le q \le q_f$, that is, $0 \le s \le 1$, and $q=\sigma_1-\sigma_3$ under triaxial stress states.

Taking Eq. (1) as the example, the wetting volumetric strain $\Delta\varepsilon_{vw}$ was only related to the confining pressure σ_3, and the wetting shear strain $\Delta\varepsilon_{sw}$ was only related to the stress level s, while it is experimentally evident that $\Delta\varepsilon_{vw}$ and $\Delta\varepsilon_{sw}$ are both highly dependent on σ_3 and s (Zhao *et al.* 2018, Zhou *et al.* 2019). In summary, these mathematical wetting models, e.g., Eq. (1), are simple and practical (Li *et al.* 2004) but are not sufficient to characterize the behavior of the wetting deformation of rockfills.

Therefore, in this paper, a series of wetting triaxial tests based on a rockfill were carried out using a large-sized triaxial apparatus. Then, the relationship between the wetting strains and stress conditions was investigated with a mathematical wetting model employed to simulate the wetting axial strain and volumetric strain under various confining pressures and stress levels. In addition, the wetting deformations of a core wall rockfill dam were analyzed by using the proposed wetting model and finite element method.

2. Test program and test results

2.1 Rockfill material

For the present study, the rockfill material was obtained from a dam located in the Henan Province in Central China (the rockfill material is hereafter called the HPR), which is rounded or subrounded sand gravel. The initial particle size distribution of the HPR is shown in Fig. 1. According to the Standard for geotechnical testing method in China (GB/T 50123, 2019), the maximum particle size used in the test should not be larger than 1/5 of the specimen diameter. Since the specimen diameter is 300 mm, the maximum particle size used in the test was set as 60 mm, and the HPR had a uniformity coefficient (C_u) of 35.6 and a curvature coefficient (C_c) of 2.26. The dry density of the specimen was 2260 kg/m^3.

2.2 Test results

The wetting triaxial test is usually adopted with two methods named “single-line” and “double-line” (Nobari and

(a) Triaxial apparatus

(b) Specimen

Fig. 3 Large-scale triaxial compression test

Table 1 Wetting test results of the specimens

σ_3 (kPa)	Items	Results				
300	Stress level s	0.00	0.22	0.42	0.79	0.90
	$\Delta\varepsilon_{1w}$ (%)	0.056	0.177	0.307	1.058	1.320
	$\Delta\varepsilon_{vw}$ (%)	0.169	0.217	0.243	0.269	0.280
600	Stress level s	0.00	0.17	0.41	0.78	0.90
	$\Delta\varepsilon_{1w}$ (%)	0.074	0.305	0.478	1.539	1.850
	$\Delta\varepsilon_{vw}$ (%)	0.223	0.270	0.352	0.385	0.400
900	Stress level s	0.00	0.19	0.40	0.77	0.90
	$\Delta\varepsilon_{1w}$ (%)	0.094	0.345	0.593	1.677	2.200
	$\Delta\varepsilon_{vw}$ (%)	0.281	0.345	0.436	0.495	0.520
1200	Stress level s	0.00	0.19	0.40	0.81	0.90
	$\Delta\varepsilon_{1w}$ (%)	0.100	0.452	0.651	1.981	2.400
	$\Delta\varepsilon_{vw}$ (%)	0.300	0.389	0.473	0.527	0.540

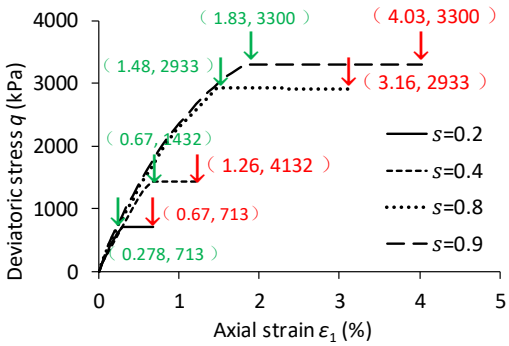

(a) Stress deviator in function of wetting axial strain

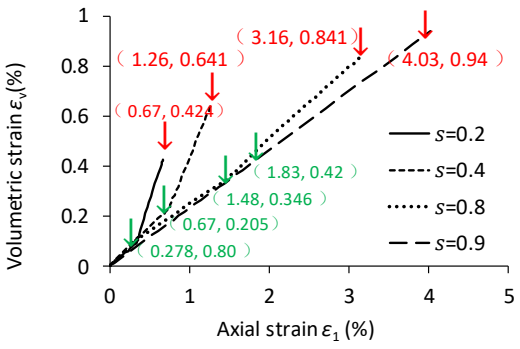

(b) Volumetric strain in function of axial strain

Fig. 4 Wetting test results of the specimens under σ_3=900 kPa at various stress levels

Duncan 1972, 1973) The "single-line" method is adopted as follows: (1) apply the required consolidation pressure to the dry specimen; (2) add axial pressure and shear the dry specimen to the designed deviatoric stress (or stress level), when the change of axial strain is less than 0.01% in 30 minutes, this step is completed, as point A shown in Fig. 2(a); and (3) wet the dry specimen to the saturated condition, and then maintain the stress condition and saturated condition until the deformation of the specimen is stable (i.e., the change of axial strain is less than 0.01% in 30 minutes), as point B shown in Fig. 2(a).

The axial strain increases from point A to point B is thought to be induced by the wetting effect, which is named the wetting axial strain, $\Delta\varepsilon_{1w}$, as shown in Fig. 2(a). The "double-line" method is adopted as follows: conduct the triaxial compression test both on the dry specimen and on the saturated specimen, as shown in Fig. 2(b), and the axial strain difference (from point C to point D) between the dry specimen and the saturated specimen at the designed deviatoric stress (or stress level) is regarded as the wetting

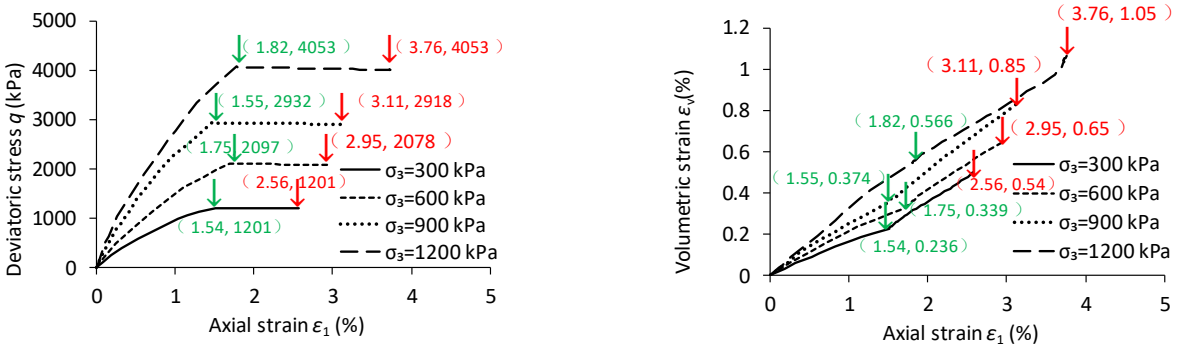

(a) Wetting axial strain (b) Wetting volumetric strain

Fig. 5 Wetting test results of the specimens under s=0.8

axial strain, $\Delta\varepsilon_{1w}$.

Since the loading and wetting steps during the "single-line" method are more similar to the construction and water storage sequences of the rockfill dam (Zuo and Shen 1989), a series of single-line wetting triaxial tests were conducted by a large-scale triaxial apparatus. Fig. 3(a) shows the large-scale triaxial apparatus. The specimen sizes were 700 mm in height and 300 mm in diameter. The HPR for one specimen, as shown in Fig. 3(b), was divided into five equal parts, and each part was compacted with a vibrator at the frequency of 60 cycles/s. The procedure was evolved after several trials to obtain the designed initial dry density.

Four different confining pressures (σ_3=300, 600, 900, and 1200 kPa) were used in the wetting triaxial test. For each given confining pressure, five typical stress levels (s=0, 0.2, 0.4, 0.8 and 0.9) were conducted. The test results were shown in Table 1.

It is noted that, even the stress levels were designed to be s=0, 0.2, 0.4, 0.8 and 0.9, respectively, the actual testing s values are only close to but not strictly equal to the design values, as shown in Table 1. Specimens under σ_3=900 kPa at s= 0.2, 0.4, 0.8 and 0.9 were taken as the examples, with the observed q-ε_1 curves and ε_v-ε_1 curves shown in Fig. 4.

In addition, the test results of the specimens under s=0.8 at σ_3= 300, 600, 900, and 1200 kPa are shown in Fig. 5. Fig 4 shows that when the confining pressure is constant, the ε_v-ε_1 curves corresponding to various s values are not same, which indicates that the wetting strains may be affected by the stress level s. Similarly, Fig. 5 shows that the wetting strains are may be affected by σ_3. In fact, the wetting test results shown in Table 1 shows that the wetting strains are affected by s and σ_3 simultaneously. Therefore, since the wetting volumetric strain $\Delta\varepsilon_{vw}$ is only related to σ_3 and wetting shear strain $\Delta\varepsilon_{sw}$ is only related to s in Eq. (1), it is not as satisfactory to express the wetting deformation behavior of rockfills.

3. Wetting deformation model

3.1 Wetting axial strain

Based on the wetting test results of all the specimens, the observed data were rearranged in terms of $\Delta\varepsilon_{1w}$ -s, as shown in Fig. 6. The relationship between $\Delta\varepsilon_{1w}$ and s was

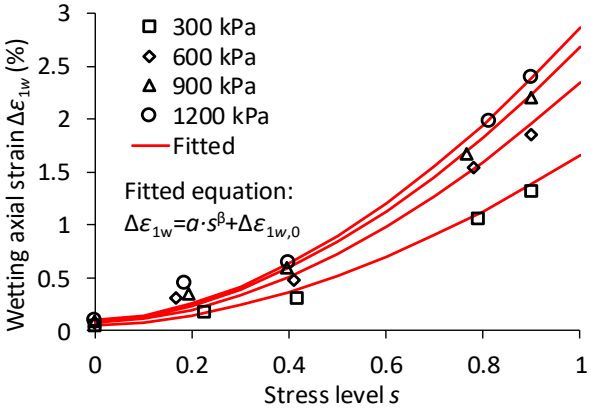

Fig. 6 Relationship between the wetting axial strain and stress level

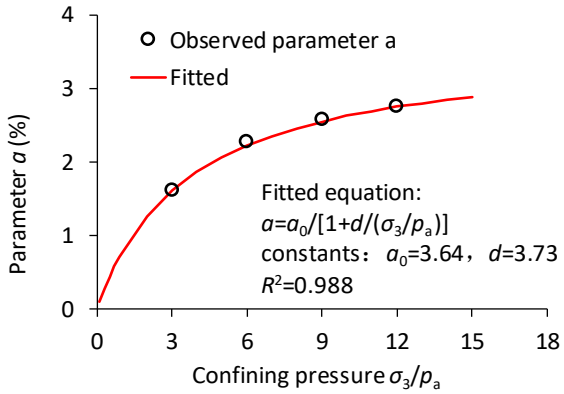

Fig. 7 Relationship between the parameter a and confining pressure

found to be well expressed as follows:

$$\Delta\varepsilon_{1w} = a \cdot s^{\beta} + \Delta\varepsilon_{1w,0} \tag{3}$$

where a and β are parameters that will be discussed below, and $\Delta\varepsilon_{1w,0}$ is the wetting axial strain under the certain confining pressure when s= 0.

The parameter β, which is 1.8 for the HPR, can be regarded as a material constant independent of the confining pressure. Meanwhile, the parameters a and $\Delta\varepsilon_{1w,0}$ were found to be related to the confining pressure. The observed parameter a and confining pressure σ_3 were plotted in the a-

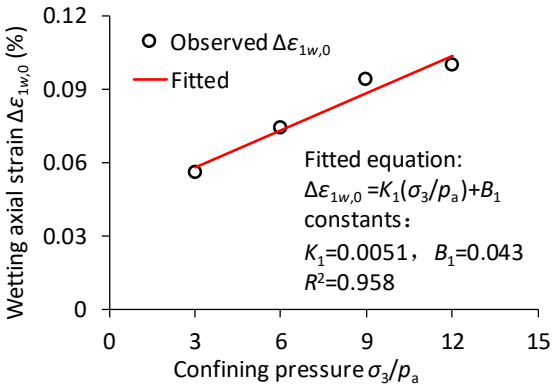

Fig. 8 Relationship between the wetting axial strain at s=0 and confining pressure

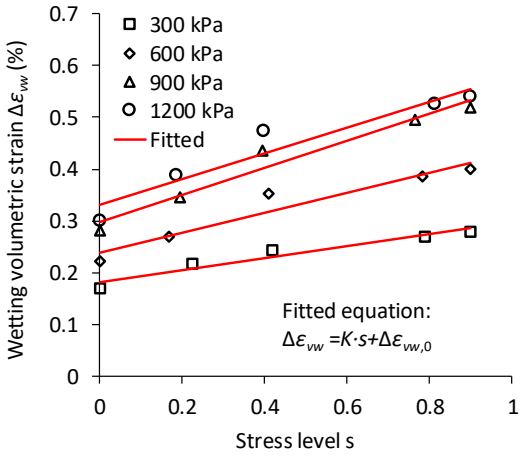

Fig. 9 Relationship between the wetting volumetric strain and stress level

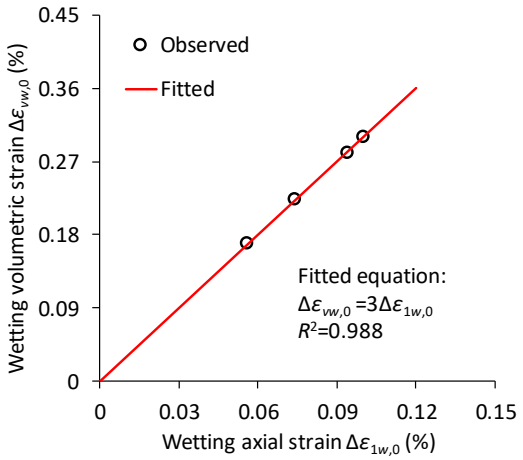

Fig. 10 Relationship between the wetting volumetric strain at s=0 and the wetting axial strain at s=0

(σ_3/p_a) plane, as shown in Fig. 6, which can be expressed as follows:

$$a=\frac{a_0}{1+d/(\sigma_3/p_a)} \tag{4}$$

where a_0 (unit: %) and d (dimensionless) are the material constants. In particular, when σ_3=0, a=0; when σ_3 is large enough, a=a_0, as the simulation line shown in Fig. 7. The material constants of the HPR are a_0=3.64 and d=3.73, and the correlation coefficient R^2 is 0.988.

The observed $\Delta\varepsilon_{1w,0}$ and confining pressure σ_3 were plotted in the $\Delta\varepsilon_{1w,0}$-(σ_3/p_a) plane, as shown in Fig. 8, which can be expressed as follows (Zhao *et al.* 2018):

$$\Delta\varepsilon_{1w,0}=K_1\cdot\left(\frac{\sigma_3}{p_a}\right)+B_1 \tag{5}$$

where K_1 (unit: %) and B_1 (unit: %) are the material constants. The material constants of the HPR are K_1=0.0051 and B_1=0.043, and the correlation coefficient R^2 is 0.958.

As a result, substituting Eqs. (4) and (5) into Eq. (2), the wetting axial strain $\Delta\varepsilon_{1w}$ under various confining pressures and stress levels can be predicted as follows:

$$\Delta\varepsilon_{1w}=\frac{a_0}{1+d/(\sigma_3/p_a)}s^{\beta}+K_1\cdot\left(\frac{\sigma_3}{p_a}\right)+B_1 \tag{6}$$

where a_0, β, d, K_1 and B_1 are the material constants.

3.2 Wetting volumetric strain

The observed wetting volumetric strain data were rearranged in terms of $\Delta\varepsilon_{vw}$ -s, as shown in Fig. 9. It is obvious that the magnitude of the volumetric strain induced by the wetting effect is larger under a higher stress level and a higher confining pressure, as shown in Fig. 9. It is easier to find out that the relationship between $\Delta\varepsilon_{vw}$ -s is linear, which has also been pointed out by Zhao *et al.* (2018). All of these properties can be reproduced as follows:

$$\Delta\varepsilon_{vw}=K\cdot s+\Delta\varepsilon_{vw,0} \tag{7}$$

where K is a parameter dependent on the confining pressure, and $\Delta\varepsilon_{vw,0}$ is the wetting volumetric strain under a certain confining pressure when s= 0. It is noted that s=0 means that the specimen is under the isotropic compression condition (σ_1 =σ_2 =σ_3, ε_1 =ε_2 =ε_3); therefore, the value of $\Delta\varepsilon_{vw,0}$ is supposed to be three times that of $\Delta\varepsilon_{1w,0}$ as follows:

$$\Delta\varepsilon_{vw,0}=3\Delta\varepsilon_{1w,0}=3\left[K_1\cdot\left(\frac{\sigma_3}{p_a}\right)+B_1\right] \tag{8}$$

where the anisotropic property of the rockfill is not considered.

Plotting the observed $\Delta\varepsilon_{vw,0}$ and $\Delta\varepsilon_{1w,0}$ of the specimens under various confining pressures in the $\Delta\varepsilon_{vw,0}$ - $\Delta\varepsilon_{1w,0}$ plane and fitting the observed data with Eq. (8), as shown in Fig. 10, it is clear that the simulation curve of Eq. (8) can describe well the relationship of the observed $\Delta\varepsilon_{vw,0}$ and $\Delta\varepsilon_{1w,0}$, with the correlation coefficient of R^2=0.988.

The parameter K is the slope of the $\Delta\varepsilon_{vw}$- s curve, as shown in Fig. 9. On the one hand, Eq. (7) can fit well with the characteristics of the observed $\Delta\varepsilon_{vw}$- s, although some data deviate slightly from the simulation line. On the other hand, the slope K was found to be directly proportional to

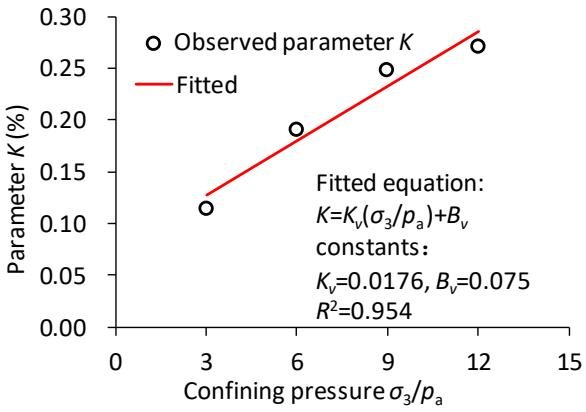

Fig. 11 Relationship between the wetting volumetric strain at s=0 and the wetting axial strain at s=0

Table 2 Wetting material constants of the rockfills

Material	a_0 (%)	β	d	K_1 (%)	B_1 (%)	K_v(%)	B_v(%)
HPR	3.64	1.8	3.73	0.0051	0.043	0.0176	0.075
Upstream rockfill	6.35	1.65	2.92	0.016	0.0196	0.0132	0.046

the confining pressure, as shown in Fig. 11. As a result, K is expressed as follows (Zhao *et al.* 2018):

$$K = K_v \cdot \left(\frac{\sigma_3}{p_a}\right) + B_v \tag{9}$$

where K_v and B_v are two material constants, and K_v=0.0176 and B_v=0.075 for the HPR.

Substituting Eq. (8) and Eq. (9) into Eq. (7), the wetting volumetric strain $\Delta\varepsilon_{vw}$ under various confining pressures and stress levels can be predicted as follows (Zhao *et al.* 2018):

$$\Delta\varepsilon_{vw} = \left[K_v \cdot \left(\frac{\sigma_3}{p_a}\right) + B_v\right] \cdot s + 3\left[K_1 \cdot \left(\frac{\sigma_3}{p_a}\right) + B_1\right] \tag{10}$$

where K_v and B_v are the material constants, and K_1 and B_1 are the same constants relating to $\Delta\varepsilon_{1w}$.

The combination of Eq. (6) and Eq. (10) is the proposed mathematical wetting model, which is believed to express the influence of the confining pressure and stress level on the wetting strains simultaneously. There are seven material constants in the proposed wetting model, i.e., a_0, β, d, K_1, B_1, K_v and B_v (the constants of the HPR are shown in Table 2), which are easily determined using wetting triaxial tests, as discussed above.

4. Case study

4.1 Dam information

In the following, the proposed wetting model and the finite element method are used to study the wetting deformation of a core wall rockfill dam. The rockfill dam example is also simulated by Lu *et al.* (2014). The maximum dam height is 160 m, the upstream and downstream of the dam slope are both 1:1.9, and the normal water level is 8 m below the dam crest. In the 3D finite element mesh, the height of the bedrock surface is 133 m, the height of the dam crest is 281 m, and the height of the normal water level is 273 m. The main material partitions are illustrated by the 2D typical cross section of the dam, which is shown in Fig. 12(a), and the 3D mesh for finite element analysis is shown in Fig. 12(b).

4.2 Constitutive model

Duncan-Chang's E-B model (Duncan and Chang 1970, Duncan *et al.* 1980) was used to analyze the stress and deformation of the dam. The tangent Young's modulus E_t and bulk modulus B were formulated as follows:

$$\begin{cases} E_t = \left[\dfrac{1-R_f(1-\sin\varphi)(\sigma_1-\sigma_3)}{2c\cos\varphi+2\sigma_3\sin\varphi}\right]^2 kp_a\left(\dfrac{\sigma_3}{p_a}\right)^n \\ B = k_b p_a \left(\dfrac{\sigma_3}{p_a}\right)^m \end{cases} \tag{11}$$

where σ_1 is the major principal stress, R_f is the failure shear stress ratio, φ is the internal friction angle, p_a is the atmospheric pressure, and k, n, k_b and m are material constants. Values of φ are better approached by a logarithmic function as follows:

$$\varphi = \varphi_0 - \Delta\varphi \log_{10}\left(\frac{\sigma_3}{p_a}\right) \tag{12}$$

where φ_0 is the internal friction angle at σ_3=100 kPa, and $\Delta\varphi$ is the reduction in friction angle for a 10-fold increase in σ_3. The main material constants of the constitutive model are listed in Table 3 after Lu *et al.* (2014). The contact behavior between the core wall and rockfill materials is simulated by using the Goodman element. In particular, relative penetration is avoided along the interface.

4.3 Wetting material constants

Eqs. (6) and (10) were used to simulate the relationship between the observed wetting strains and the confining pressure and stress level, which are illustrated in Fig. 13, with the obtained wetting material constants shown in Table 3. Fig. 13 shows that the simulations of Eqs. (6) and (10) can estimate well the observed wetting strains of the upstream rockfill (sharp angular fill material), which indicates that the proposed wetting model is applicable to express the wetting deformation behavior of the rockfills. Furthermore, the determined wetting material constants are reasonable for use in finite element analysis.

4.4 Wetting deformation

The upstream rockfill is located inside the reservoir and is therefore subjected to the rising water level. The material of the core wall is compacte with highly plastic clay, and its permeability is much less than that of the rockfills. Meanwhile, the function of the core wall, which can be regarded as an impervious core, is to prevent seepage. Thus,

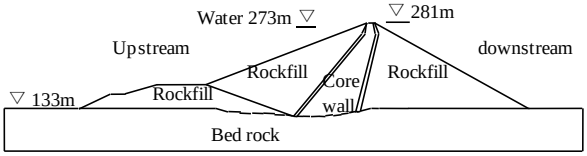

(a) Typical cross section and main material partitions of the dam

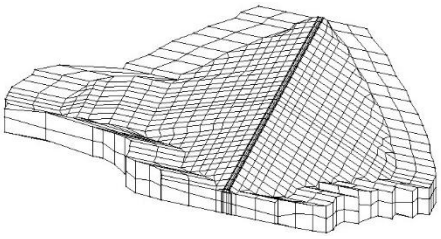

(b) 3D mesh

Fig. 12 Necessary information of the dam

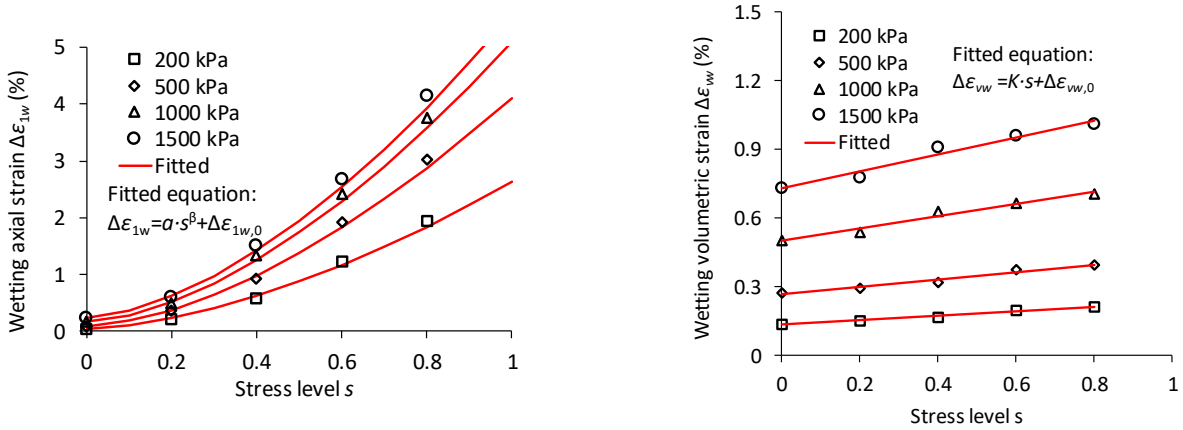

(a) Wetting axial strain

(b) Wetting volumetric strain

Fig. 13 Observed and simulated wetting strains of the upstream rockfill

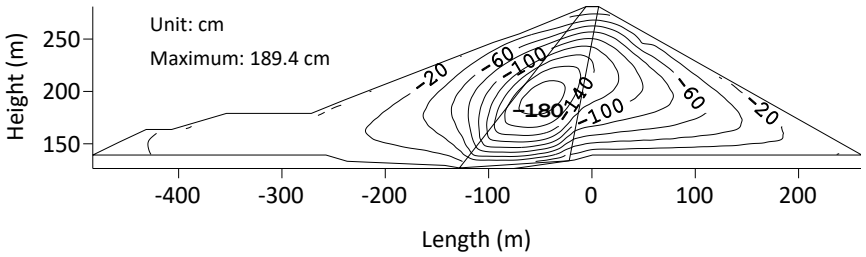

(a) Contours of vertical settlement

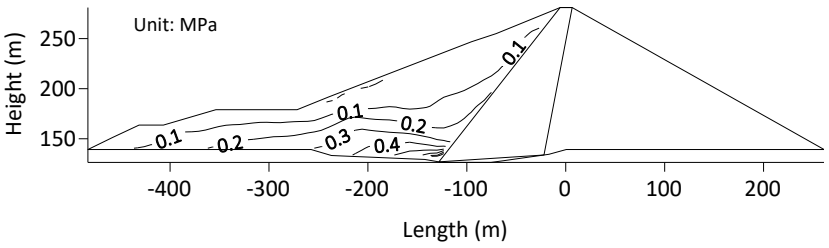

(b) Contours of the minor principal stress in the upstream rockfill

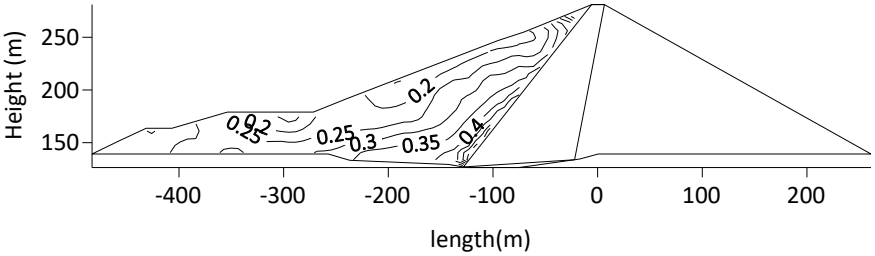

(c) Contours of the stress level in the upstream rockfill.

Fig. 14 Results of the finite element analysis after water storage (without considering the wetting effect)

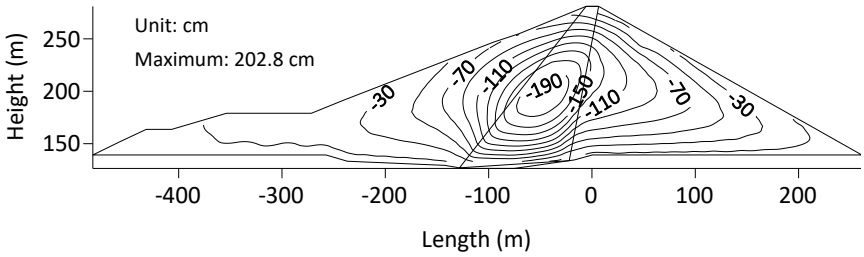

(a) Settlement of the dam

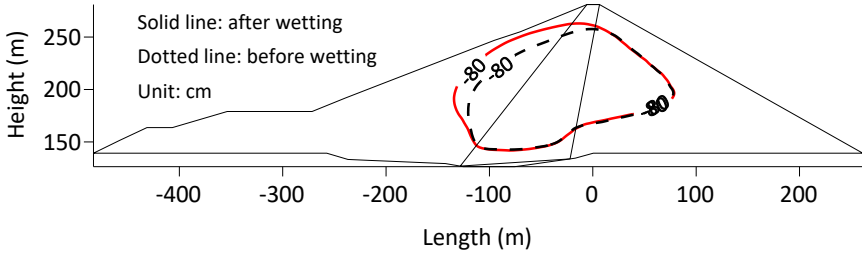

(b) Contours of -80 cm before and after wetting

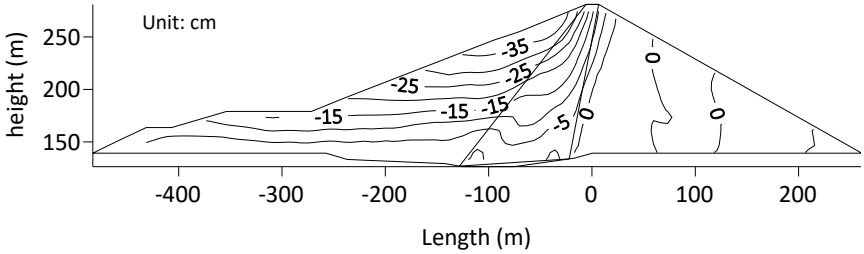

(c) Additional settlement induced by the wetting effect

Fig. 15 Deformation of the dam considering the wetting effect

it is believed that the water in the reservoir cannot pass through the core wall, and as a result, it is assumed that the wetting effect only occurs in the upstream rockfill, and the core wall and downstream rockfill are not affected.

Two numerical schemes were designed in the finite element analysis. The first scheme is the original one without considering the wetting effect. The horizontal expansion, vertical contraction and stress condition of the dam after adding a multistage water load (that is, the filling of the reservoir to a height of 273 m) were calculated using Duncan-Chang's E-B model. The water level rose from 133 m (Bedrock surface) to 273 m, and the rising height of water level is 140 m. Therefore, 14 water rising steps were designed to model the process of water level rising, and one step corresponds to 10 m increment in water level. In every step, the hydrostatic pressure (including water buoyancy) has been considered by acting at the upstream rockfill and upper boundary of the impervious core wall.

The other scheme is the so-called wetting scheme. It should be noted that the hydrostatic pressure and wetting effect occur simultaneously in the process of water storage, both of which influence the deformation of the dam. Based on the original scheme, each water rising step was followed by a wetting step, as a result, 14 wetting steps were designed in this scheme. For example, when the water level rises from 133 m to 143 m in the first water level rising step, the hydrostatic pressure will be calculated firstly, and then, the stress condition will be submitted into Eq. (6) and Eq. (10). The additional deformation induced by the wetting effect can be calculated, which is the so-called first wetting step. After the first wetting step, the stress and strain conditions will be Iterated to the second water level rising step, an in the same way, the other 13 wetting steps can be carried out orderly.

The vertical settlement was taken as the example to show the deformation induced by the wetting effect. The contours of the vertical settlement after adding the water load, i.e., the results of first scheme, are shown in Fig. 14(a), and the maximum settlement, 189.4 cm, occurs under the middle of the core wall. The contours of the minor stress σ_3 and stress level s in the upstream rockfill after adding the water load are shown in Fig. 14(b) and Fig. 14(c), respectively. Fig. 14 shows that the minor stress and stress level both increase with increasing depth. The maximum stress level is approximately 0.8, and the maximum minor stress is approximately 1200 kPa, both of which occur around the bottom of the upstream rockfill next to the core wall.

The contours of the vertical settlement considering the wetting effect, i.e., the results of wetting scheme are shown in Fig. 15(a), and the maximum vertical settlement increases to 202.8 cm according to the results. It is difficult to tell the difference induced by the wetting from Fig. 14(a) and Fig. 15(a) directly, except for the notably different maximum settlements. Therefore, the contours of -80 cm before and after wetting were taken as the example, as

shown in Fig. 15(b). On the one hand, in the upstream rockfill, it is clear that the contour of -80 cm after wetting is above that before wetting, which means that the vertical settlement of the upstream rockfill is increased after wetting. On the other hand, in the core wall and downstream rockfill, the contours of -80 cm before and after wetting are nearly the same because the wetting in these parts were not considered.

In addition, to clearly show the influence of the wetting effect on the deformation of the dam, the displacement induced by the wetting effect on the dam is shown in Fig. 15(c). The additional settlements are mainly concentrated in the upstream and core-wall parts; the maximum additional settlement, 37.2 mm, occurs near the upstream slope and the maximum vertical settlement occurs at the crest, which indicates that the influence of the wetting effect is considerable. In summary, the applicability of the proposed wetting model has been preliminarily verified, although there are no field measurements for comparison.

5. Conclusions

In this paper, the wetting deformation behavior of rockfill material was studied. The wetting strains, including the wetting axial strain and wetting volumetric strain, were both found to increase with increasing confining pressure and stress level. Therefore, the relationships between the wetting strain characteristics and stress conditions have been obtained, which is regarded as the wetting model. The wetting deformation of a core wall rockfill dam was studied by the proposed wetting model and the finite element method. On the one hand, the capacity of the proposed wetting model is shown by good agreement of the results obtained from the simulation with the wetting test data of the upstream rockfill of the dam. On the other hand, the wetting deformation predicted by the model is reasonable, which indicates the potential of the model in dam engineering.

Acknowledgments

The authors gratefully acknowledge the financial support from the Key Laboratory of Ministry of Education for Geomechanics and Embankment Engineering, the Fundamental Research Funds for the Central Universities (No. B2002040320), the Yalong River Joint Fund of National Natural Science Foundation of China and the Yalong River Hydropower Development Company, Ltd. (No. U1865103).

References

Ameen, A.M.S., Ibrahim, Z. and Othman, F. (2017), "Three-dimensional seismic response analysis for a rockfill dam", *J. Comput. Theor. Nanosci.*, **14**(12), 6003-6013. https://doi.org/10.1166/jctn.2017.7048.

Bauer, E., Fu, Z.Z. and Liu, S.H. (2010), "Hypoplastic constitutive modelling of wetting deformation of weathered rockfill materials", *Front. Archit. Civ. Eng. China*, **4**(1), 78-91. https://doi.org/10.1007/s11709-010-0011-8.

Chen, X.Y., Yan, H.Z. and Liu, X.X. (2011), "Study on engineering characteristics of highly weathered weak rock", *Adv. Mater. Res.*, **261-263**, 1309-1312. https://doi.org/10.4028/www.scientific.net/AMR.261-263.1309.

Duncan, J.M. and Chang, C. (1970), "Nonlinear analysis of stress and strain in soils", *J. Soil Mech. Found. Div.*, **96**(SM5), 1629-1653.

Duncan, J.M., Byrne, P., Wong, K. and Marbry, P. (1980), "Strength, stress strain and bulk modulus parameters for finite element analyses of stresses and movements in soil masses", University of California, Berkeley, California, U.S.A.

Escuder, I., Andreu, J. and Rechea, M. (2005), "An analysis of stress-strain behaviour and wetting effects on quarried", *Can. Geotech. J.*, **42**(1), 51-60. https://doi.org/10.1139/t04-071.

Fu, Z.Z., Liu, S.H. and Gu, W.X. (2011), "Evaluating the wetting induced deformation of rockfill dams using a hypoplastic constitutive model", *Adv. Mater. Res.*, **243-249**, 4564-4568. https://doi.org/10.4028/www.scientific.net/AMR.243-249.4564.

GB/T 50123. (2019), *Standard for Geotechnical Testing Method*, China Planning Press, Beijing, China. (in Chinese)

Karalar, M. and Cavusli, M. (2019), "Examination of 3D long-term viscoplastic behaviour of a CFR dam using special material models", *Geomech. Eng.*, **17**(2), 119-131. https://doi.org/10.12989/gae.2019.17.2.119.

Li, G., Wang, L. and Mi, Z. (2004), "Research on stress-strain behaviour of soil core rockfill dam", *Chin. J. Rock Mech. Eng.*, **23**(8), 1363-1369 (in Chinese).

Lu, Y.Y., Gao, Z.P. and Zhu, J.G. (2014), "Effect of wetting deformation on behavior of earth rockfill dam", *J. Yangzhou Univ. Nat. Sci. Ed.*, **17**(3), 64-68, 73 (in Chinese).

Nobari, E.S. and Duncan, J.M. (1972), "Effect of reservoir filling on stresses and movements in earth and rockfill dams", No. TE-72-1, University of California, Berekely, U.S.A.

Nobari, E.S. and Duncan, J.M. (1973), "Movements in dams due to reservoir filling", *Proceedings of the ASCE Specialty Conference on Performance of Earth and Earth -supported Structure*, Lafayette, Pennsylvania, U.S.A.

Oldecop, L.A. and Alonso, E. (2007), "Theoretical investigation of the time-dependent behaviour of rockfill", *Geotechnique*, **57**(3), 289-301. https://doi.org/10.1680/geot.2007.57.3.289.

Pramthawee, P., Jongpradist, P. and Sukkarak, R. (2017), "Integration of creep into a modified hardening soil model for time-dependent analysis of a high rockfill dam", *Comput. Geotech.*, **91**, 104-116. https://doi.org/10.1016/j.compgeo.2017.07.008.

Raisianzadeh, J., Mohammadi, S. and Mirghasemi, A.A. (2019), "Micromechanical study of particle breakage in 2D angular rockfill media using combined DEM and XFEM", *Granul. Matter*, **21**(3), 48. https://doi.org/10.1007/s10035-019-0904-8.

Reza, M., Ali, A. and Behrouz, G. (2015), "Simulation of collapse settlement of first filling in a high rockfill dam", *Eng. Geol.*, **187**, 32-44. https://doi.org/10.1016/j.enggeo.2014.12.013.

Sukkarak, R., Pramthawee, P., Jongpradist, P., Kongkitkul, W. and Jamsawang, P. (2018), "Deformation analysis of high CFRD considering the scaling effects", *Geomech. Eng.*, **14**(3), 211-224. https://doi.org/10.12989/gae.2018.14.3.211.

Wang, T., Liu, S. and Lu, Y. (2019), "Laboratory experiments on the improvement of rockfill materials with composite grout", *Geomech. Eng.*, **17**(3), 307-316. https://doi.org/10.12989/gae.2019.17.3.307.

Xiao, Y. and Liu, H. (2017), "Elastoplastic constitutive model for rockfill materials considering particle breakage", *Int. J. Geomech.*, **17**(1), 04016041. https://doi.org/10.1061/(ASCE)GM.1943-5622.0000681.

Zhao Z. L., Zhu J.G., Du Q. and Al Sakran, M.A. (2018), "Wetting deformation of coarse-grained materials in triaxial test", *Hydro*

Sci. *Eng*., (6), 84-91 (in Chinese).
Zhou, X., Chi, S. and Jia, Y. (2019), "Wetting deformation of core-wall rockfill dams", *Int*. *J*. *Geomech*., **19**(8), 4019084. https://doi.org/10.1061/(ASCE)GM.1943-5622.0001444.
Zuo Y.M. and Shen Z.J. (1989), "Determination of deformation character of gravel sand due to wetting", *Hydro Sci*. *Eng*., (1), 107-113 (in Chinese).

IC